

# Lightweight Deployable Thin Shell-membrane W-band Reflector for SmallSats

Principal Investigator: Paolo Focardi (337); Co-Investigators: Juan Mejia-Ariza (353), Lynn Long (353), Eric Marin (UCLA), Igor M. De Rosa (UCLA), Jenn-Ming Yang (UCLA)

Program: FY21 SURP

Strategic Focus Area: Climate Science

## Objective

The UCLA/JPL team planned to develop suitable materials for a 1.5m thin shell-membrane W-band deployable reflector, based on requirements consistent with a SmallSat application for Earth and/or planetary science projects. The proposed antenna design is comprised of a thin RF shell-membrane embedded into a substrate backing material that will allow high stowing efficiency inside a target volume of 6U or less. Since this task was funded for only one year we focused our efforts on material developments and explored the RF and mechanical properties of the proposed materials for the reflector surface. The group of Prof. Jenn-Ming Yang at UCLA has done a lot of work in the field of material development and is best suited to tackle this material challenge with the guidance of JPL on materials for space applications. They achieved outstanding results in a relatively short time and with extremely limited resources. The collaboration between JPL and UCLA has enhanced JPL knowledge and expertise in the area of large deployable high gain antennas for SmallSats. In addition, this collaboration has provided an opportunity for a student to make a significant contribution to this field of research.

## Significance/Benefits to JPL and NASA

W-band reflectors have never flown on SmallSats. The development of a W-band (94 GHz) radar system directly addresses NASA strategic plans as an enabling technology to target the Clouds, Convection and Precipitation science, one of the highest priority observables identified by the Earth Science and Applications from Space Decadal Survey. The development of high-frequency light-weight antennas directly addresses two major JPL strategic plans as enabling *miniaturized systems* and *advanced manufacturing, design and materials* that will make possible new missions previously considered cost-prohibited and technically unfeasible for planetary exploration, Earth science, or space-based astronomy. With the advances in material development shown by this work we are now a step closer in making deployable W-band reflector a reality. The RF and mechanical performance shown by both the Carbon Nano Tube approach and the Graphene Oxide/Polyimide approach are extremely promising and set the basic processes and procedures to improve these materials in the future.

## Acknowledgments

The authors would like to acknowledge Eric Marin for his ingenuity, dedication and enthusiasm in developing the GO/PI & GO/PDA approach up until the very last day. His relentless support for this task was greatly appreciated. The authors would also like to thank Dr. Igor M. De Rosa for his help on the front of CNT sheet development and processing. His skills and expertise were fundamental in achieving the results shown in this work.

## Background

The large deployable mesh reflectors used for the Soil Moisture Active/Passive (SMAP) and the NASA ISRO SAR (NISAR) missions were designed to operate at L-band or S-Band frequencies. These mesh reflectors are made of a conductive grid net (knitted, gold-plated, molybdenum wire mesh) coupled with a complex supporting deployable structure. Due to the very low stiffness of the mesh, attempting to force it into a paraboloid shape by controlling it only at a small number of points results in surface and shape accuracy errors not tolerable at W-band. Current state of the art for Ka-band deployable mesh reflector is the Raincube antenna, but its architecture cannot be used at higher frequencies. With this work we aimed at developing, at the material level, large deployable reflectors with surface accuracy and thermal stability suitable for W-band applications or even higher frequencies. This will allow low cost large reflectors to be deployed on small platforms and allow science applications that are cost-prohibited today.

## Approach and Results

Two approaches were undertaken to achieve flexible ultra-high-conductivity films: one utilizing a carbon nanotube (CNT) sheet substrate deposited with gold nano-particles, the other created from a chemically altered and graphitized graphene oxide film. The first approach increased the electrical conductivity of these materials from  $\sim 1 \times 10^4$  S/m to  $4 \times 10^6$  S/m, a 410-fold increase, as the result of two unique gold nanoparticle self-assembly processes. The gold film formed by one of these processes demonstrated an electrical conductivity of  $2.4 \times 10^7$  S/m when measured independently of the CNT sheet substrate. The CNT sheets also demonstrated an anti-wrinkle and shape memory effect that would aid in deployment actuation. The second approach led to the creation of multiple novel nano-carbon composites that are still being evaluated.

Fig. 1 outlines the process chronology and conductivity evolution, and introduces the “gold deposition” and “gold electroless plating” processes. The former produces spherical nanoparticles (Fig.2), while the latter produces a uniform and continuous thin film. Thickness can be varied from the nanometer to micron scale by controlling solution concentration and exposure time. X-ray diffraction (XRD) was used to evaluate the crystal structure and composition of the gold film. The diffraction pattern (Fig. 3) corresponds to that of polycrystalline gold having a face-centered cubic lattice, primarily in the (111) orientation, and does not indicate the presence of any intermetallic gold compounds. Energy dispersive X-ray spectroscopy (EDS) and X-ray photoelectric spectroscopy (XPS) identified the presence of gold, carbon, and oxygen, congruent with surface oxidation and slight handling contamination of the XPS samples. Digital scanning calorimetry determined the melting point of the film to be 1061 °C, which compared to pure gold (1064 °C) further supporting the purity of the gold film. Several samples representative of candidate reflector materials comprised of CNT sheets with different gold treatment combinations were delivered to JPL for high frequency (W-band/90 GHz) reflection measurements in waveguide. Electrical conductivities ranged from  $6.5 \times 10^5$  S/m to  $4.2 \times 10^6$  S/m, while areal densities ranged between 29 and 71 g/m<sup>2</sup> and total film thicknesses ranged between 10 and 20  $\mu$ m, not respectively. Results from these tests are currently pending.

Due to equipment limitations resulting from the ongoing pandemic the focus of the graphene approach was shifted from graphene oxide/polyimide (GO/PI) films to graphene oxide/polydopamine (GO/PDA) films. GO/PDA has been shown to exhibit increased thermal conductivity over GO/PI, electrical conductivity approaching the  $10^6$  S/m range, and rapid cycle times through simple aqueous chemistry. Samples with improved film continuity are under fabrication. CNT sheet/PDA composites were also fabricated with the goal of creating continuous and highly-conductive non-metallic films as an alternative to the gold treatments. Resulting PDA structures are detailed in Fig. 4, where discontinuous but mostly uniform films were created along with PDA nanoparticles embedded in the CNT sheet itself. Initial XRD analysis shows the creation of a highly ordered, oxidized graphene-like film with the addition of PDA from the peak at 14.38° (Fig.5), that is then chemically reduced by the annealing process. Further characterization is pending.

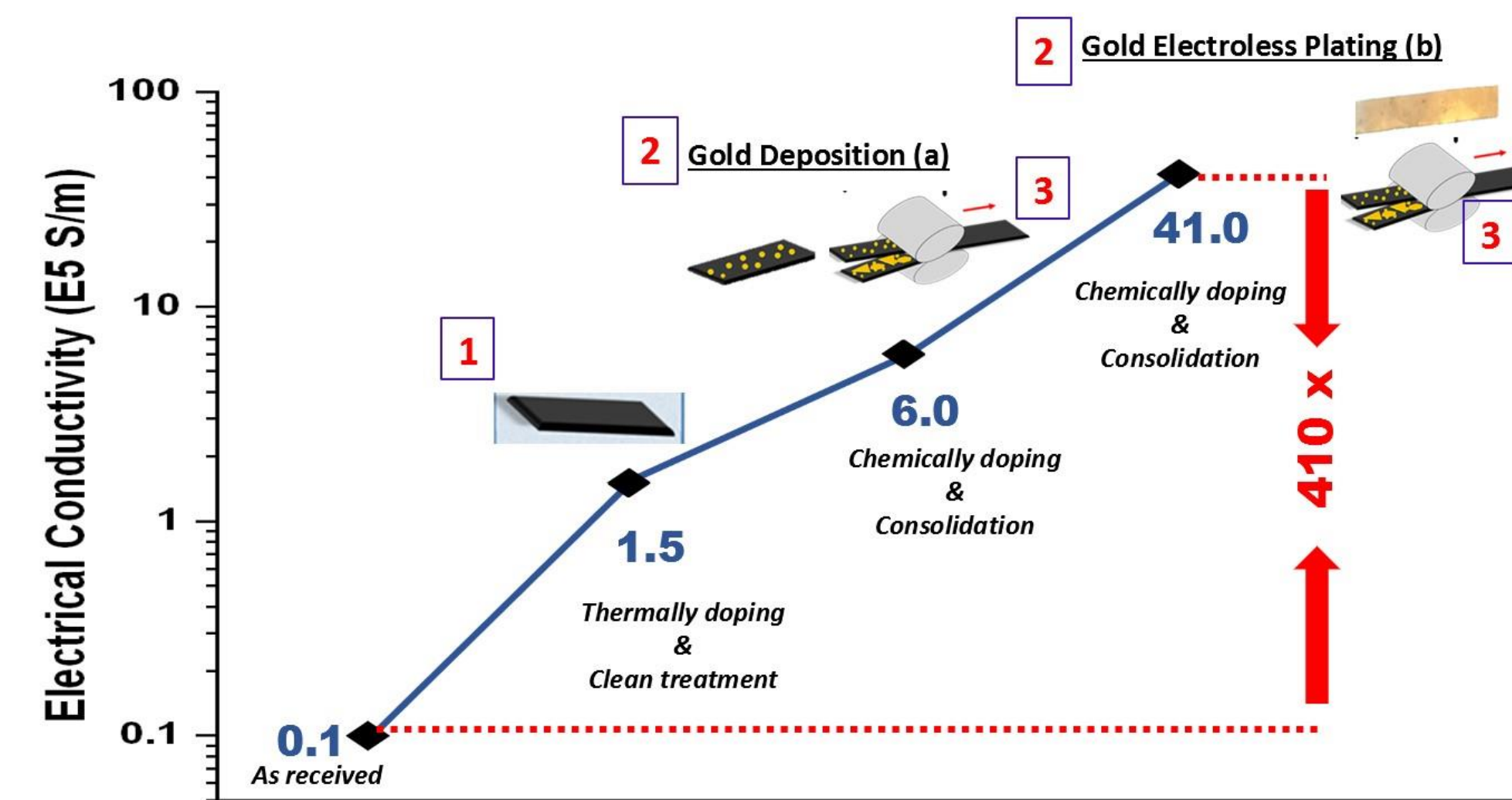


Figure 1, Multi-step treatment for conductivity improvement and the resultant conductivity values

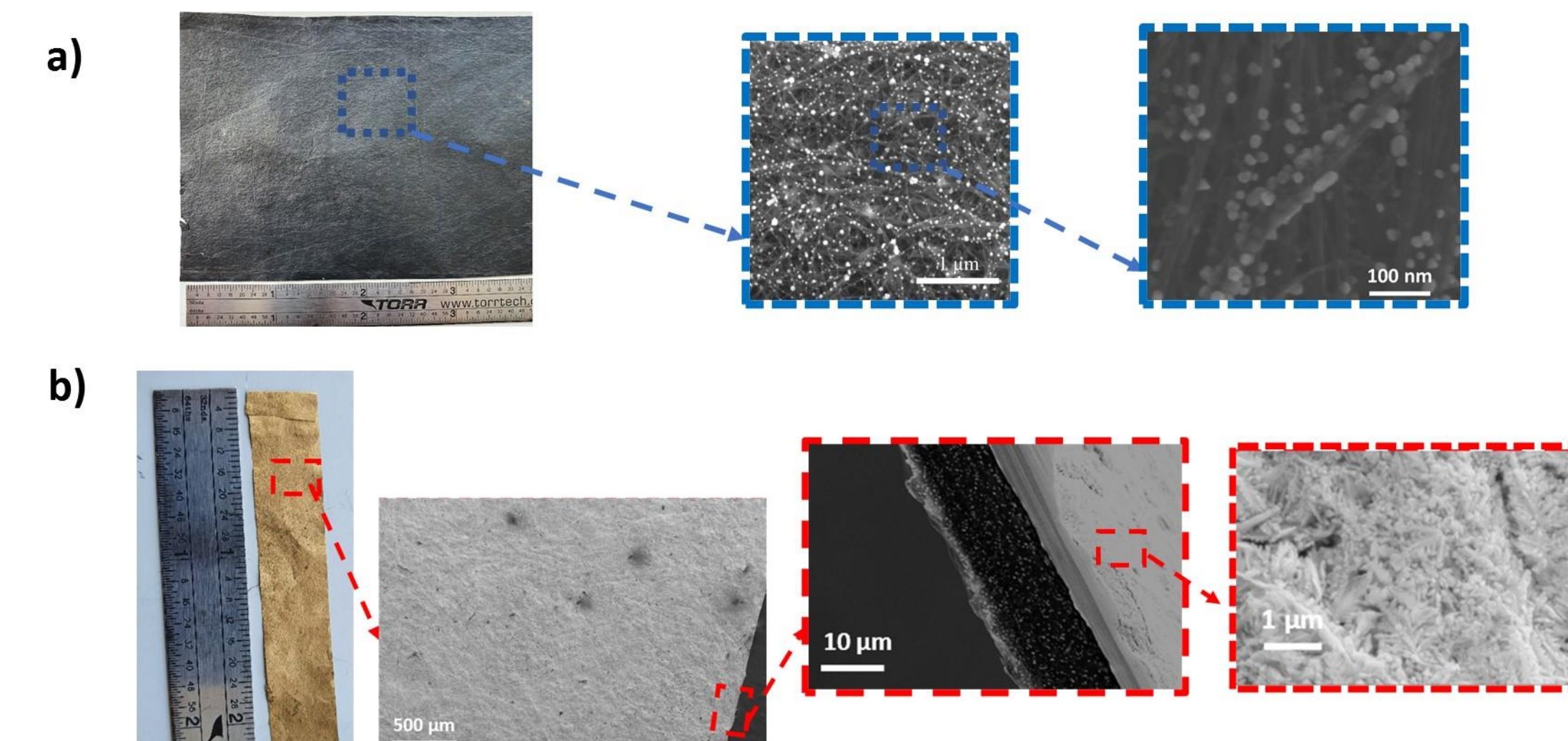


Figure 2, SEM images of the morphology of the surface and cross-section of CNT film after (a) gold “deposition” (b) gold “electroless plating”

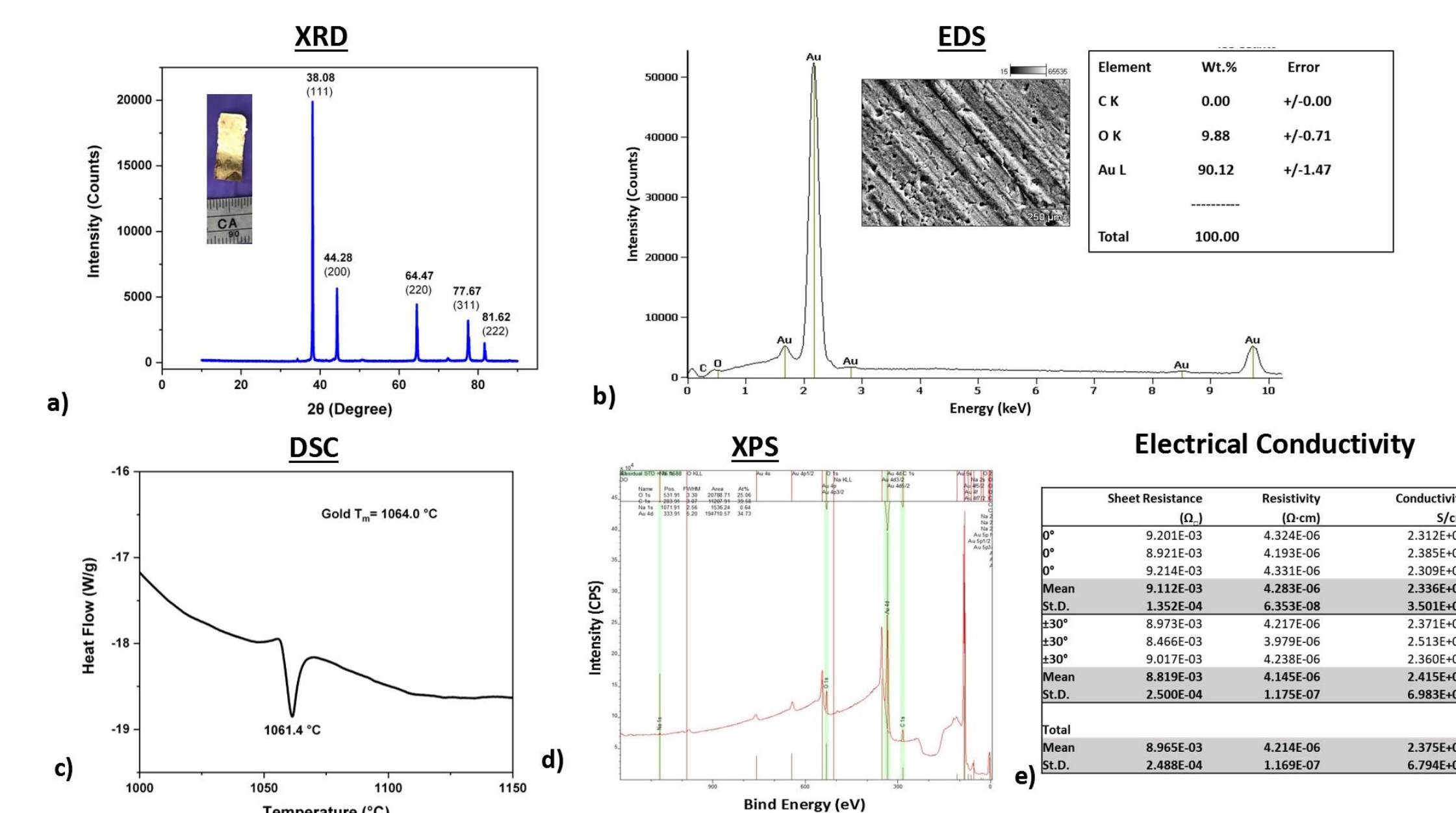


Figure 3, XRD pattern (a), EDS analysis (b), DSC analysis (c), XPS spectrum (d), Electrical Conductivity values (e) of gold film having a thickness of 2  $\mu$ m

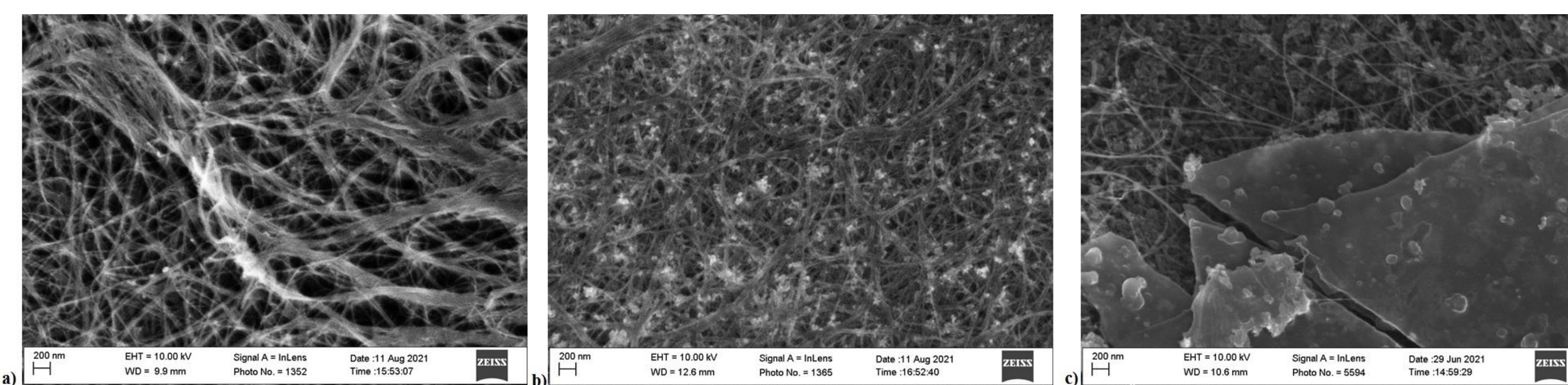


Figure 4, SEM images of (a) clean CNT sheet, (b) PDA particles embedded in CNT sheet, and (c) PDA film on top of CNT sheet

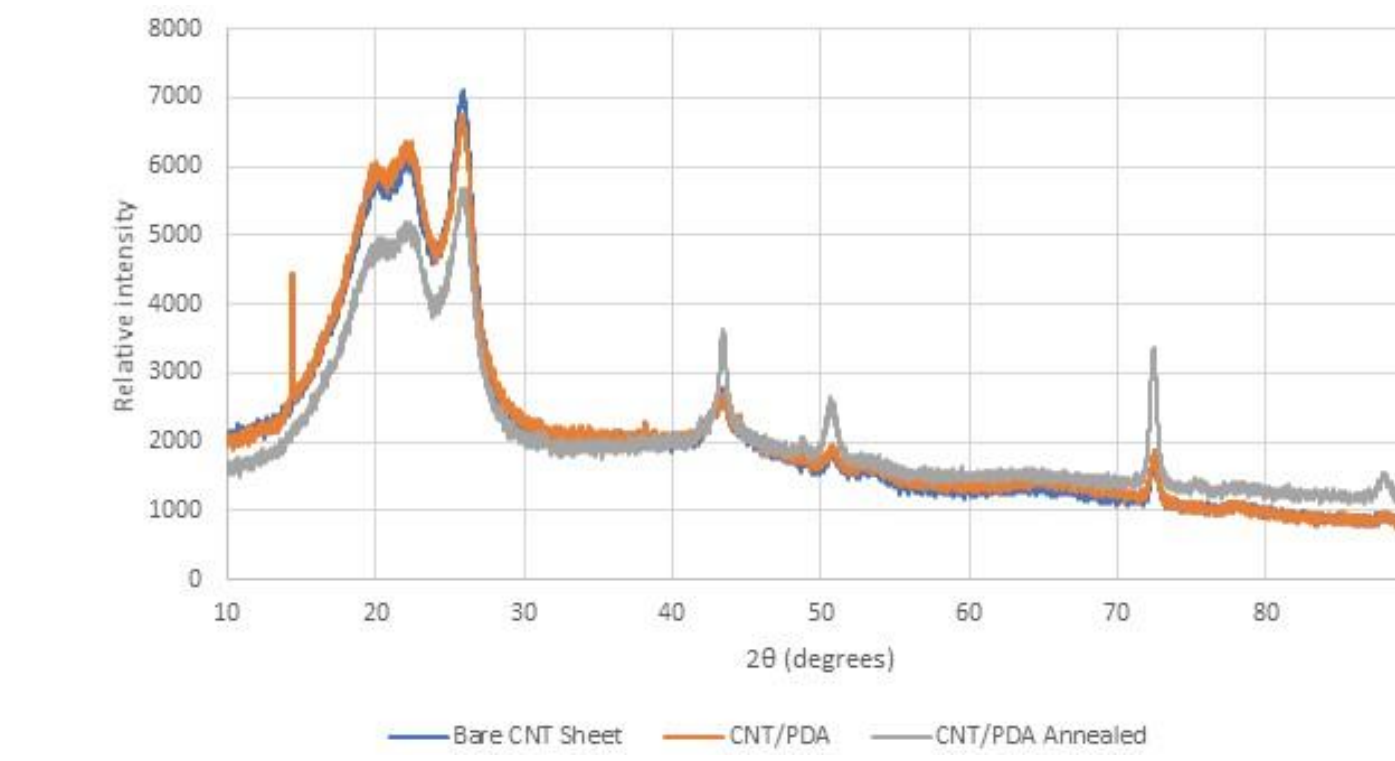


Figure 4, X-ray diffraction pattern of as-cleaned CNT sheet, CNT sheet after PDA deposition, and CNT/PDA composite after thermal annealing/carbonization

## References

- P. Ye, W. Xin, I. M. De Rosa, Y. Wang, M. Goorsky, L. Zheng, X. Yin, Y. H. Xie, “One-Pot Self-Templated Growth of Gold Nanoframes for Enhanced Surface-Enhanced Raman Scattering Performance. ACS Applied Materials & Interfaces, 12, 19, 22050-22057, 2020.
- W. Xin, I. M. De Rosa, Y. Cao, X. Yin, H. Yu, P. Ye, L. Carlson and J. M. Yang, “Ultrasonication-assisted Synthesis of High Aspect Ratio Gold Nanowires on Graphene Template and Investigation of Their Growth Mechanism”. Chem. Commun, 54 (33), 4124-4127, March 2018.
- W. Xin, J. Severino, I. M. De Rosa, D. Yu, J. McKay, P. Ye, X. Yin, J.M. Yang, L. Carlson, and S. Kodambaka, “One-Step Synthesis of Tunable-Size Gold Nanoplates on Graphene Multilayers”. ACS Nanoletters, 18 (3), 1875-881, February 2018.
- W. Xin, I. M. De Rosa, P. Ye, J. Severino, C. Li, X. Yin, M.S.Goorsky, L. Carlson, J.M. Yang, “Graphene Template Induced Growth of Single-crystalline Gold Nanobelt with High Structural Tunability”. Nanoscale, 10, 2764-2773, 2018.
- W. Xin, J.M. Yang, C. Li, M.S.Goorsky, L. Carlson, I. M. De Rosa, “Novel strategy for one-pot synthesis of gold nanoplates on carbon nanotube sheet as an effective flexible sers substrate”. ACS applied materials & Interfaces, 9(7), 6246-6254, January 2017.

National Aeronautics and Space Administration

Jet Propulsion Laboratory  
California Institute of Technology  
Pasadena, California

www.nasa.gov